Nature Environment and Pollution Technology
An International Quarterly Scientific Journal

p-ISSN: 0972-6268
e-ISSN: 2395-3454

Vol. 18 | No. 4 | pp. 1211-1218 | 2019

Original Research Paper | Open Access

Retrieval of the Canopy Chlorophyll Density of Winter Wheat from Canopy Spectra Using Continuous Wavelet Analysis

Qingkong Cai*, Erjun Li†, Jiechen Pan* and Chao Chen***

*College of Civil Engineering, Henan University of Engineering, Zhengzhou, Henan 451191, China
**College of Human and Social Sciences, Henan University of Engineering, Zhengzhou, Henan 451191, China
†Corresponding author: Erjun LI

Nat. Env. & Poll. Tech.
Website: www.neptjournal.com

Received: 15-09-2019
Accepted: 18-10-2019

Key Words:
Canopy chlorophyll density
Continuous wavelet analysis
Winter wheat
Spectral indices
Hyperspectral remote sensing

ABSTRACT

Continuous wavelet analysis (CWA) has been applied to leaf-scale spectral data for quantifying leaf chlorophyll content, but its application to canopy-scale spectral data for estimating the canopy chlorophyll density (CCD) of winter wheat at different growth stages requires further analysis. This study aims to estimate CCD by applying CWA to the canopy spectra of 185 samples from Guanzhong Plain, China. The five most informative wavelet features related to CCD were identified using the CWA method. Meanwhile, 10 commonly used spectral indices were selected to compare with the CWA method. Two partial least square regression (PLSR) models based on wavelet features and spectral indices were developed and compared. Results showed that the PLSR model using wavelet features (R^2 = 0.64, RMSE = 0.43 g/m^2) was better than that using spectral indices (R^2 = 0.57, RMSE = 0.48 g/m^2) and wavelet features were less sensitive to the growth stage variation than spectral indices. This result suggested that the CWA approach can derive robust wavelet features and was more effective than spectral indices for predicting CCD from canopy-scale spectral data for an agricultural ecosystem.

INTRODUCTION

Accurate quantitative estimates of key biophysical variables are crucial for land surface models that quantify the exchange of energy and matter between the land surface and lower atmosphere (Houborg et al. 2008). Key biophysical variables include the canopy chlorophyll density (CCD), which is defined as the total amount of foliage pigment per unit ground area, that assists in determining photosynthetic capacity and predicting productivity (Nijs et al.1995). Therefore, an accurate monitor of CCD is significant for precise agriculture fertilization, which can effectively avoid the gradual decline of ecological environment caused by the excessive inputs of chemical fertilizer.

Remote sensing techniques for estimating vegetation biophysical variables have been based on either the empirical statistical approach that relates canopy variables to single spectral reflectance or vegetation indices (VIs) or the inversion of a physically based model (Boegh et al. 2002, Houborg et al. 2008). The VI approach is highly preferred for large-scale remote sensing applications due to its simplicity. Previous studies have shown that reflectance in the green, red, red edge, and near-infrared spectral regions is sensitive to a wide range of chlorophyll content in leaves and canopies (Colombo et al. 2003). VIs based on these spectral regions have been used successfully (Gitelson et al. 2005). However, the spectral index approach has apparent limitations. On the one hand, spectral indices use only two or three wavebands, not the entire spectral information provided from a reflectance curve. On the other hand, spectral reflectance relationships are site-, time-, and crop-specific, making the use of a single relationship for an entire region unfeasible (Houborg et al. 2008, Buschmann et al. 1993). The physically based model describes the transfer and interaction of radiation inside the canopy on the basis of physical laws and thus provides an explicit connection between the biophysical variables and canopy reflectance. However, this method is computationally intensive and complex and has an ill-posed nature of model inversion (Gitelson et al. 1996), thereby limiting its widespread practical use.

Continuous wavelet analysis (CWA) can decompose reflectance spectra into a number of scale components and permits the extraction of wavelet features that capture useful spectral information pertinent to quantifying forest biophysical parameters, leaf water content, and leaf chlorophyll content (Gitelson et al. 1996, Daughtry et al. 2000, Dash et al. 2004). However, previous research is limited by applying CWA to leaf reflectance spectra measured in laboratories and simulated with radiative transfer models (Daughtry et al. 2000, Atzberger 2004). Meanwhile, the efficiency of the CWA approach in estimating the CCD of winter wheat at

different growth stages from the canopy spectra still requires further study. The canopy spectra are more complex than the leaf spectra due to a number of complicating factors, such as soil background and canopy structural variation (Broge et al. 2002), which make CCD retrieval challenging. In addition, although several studies have established models for estimating CCD, most of them have focused on using single growth stage data and have not validated the sensitivity of their methods to the growth stage variation in canopy spectra, thereby limiting the widespread application of their methods.

The present study aims to investigate the spectroscopic estimation of CCD by applying the CWA method to the canopy spectra of 185 winter wheat samples from two growth stages. We apply two partial least square regression (PLSR) models based on the most informative wavelet features and optimal spectral indices to validate the sensitivity to the growth stage variation of winter wheat in CCD compared with field measurements. Specifically, the objectives of this study are as follows: (1) to select the spectral region that is sensitive to chlorophyll content and (2) to propose a strategy for improving the estimation accuracy of chlorophyll content.

DATA COLLECTION

Study Area

The three core experiment sites, namely, Juliang, Xinglin, and Rougu, are located in the Guanzhong Plain of Shanxi Province, China. They cover areas of 2.33, 6.67, and 2.00 km^2, respectively. The altitude ranges from 325 m to 800 m. The area has a monsoon climate with a hot summer and cool winter. The mean annual temperature is 12.9°C, and the mean annual precipitation is 635.1 mm with marked seasonal variations. Winter wheat is the main crop type in the area, and the main soil types are loam, clay loam, and medium. The entire growth period of winter wheat is 225 days.

Two field measurements were conducted at the growth cycle of winter wheat in 2013: one in the jointing stage (from March 31 to April 1 of 2013) and the other in the grain filling stage (from May 27 to May 28 of 2013). Sample sites were selected where soil and canopy conditions were fairly homogeneous in surrounding areas on scales of tens of meters and where the vegetation appeared healthy and capable of surviving through the experiment. The coordinate of each site was recorded with a differential GPS (Trimble 332, USA).

Canopy Hyperspectral Measurements

Canopy spectra were measured using an ASD FieldSpec FR spectroradiometer (ASD, Boulder, USA) ranging 350-2500 nm between 10:00 a.m. and 14:00 p.m. in local time (GMT+8), when the sky was slightly cloudy or had no cloud. Care was taken to avoid measuring the canopy spectra while the clouds were passing overhead. The detector was positioned vertically downward from a height of 50 cm upon the canopy. Before the canopy spectra were collected, the instrument was optimized and calibrated with a white panel (99% reflectance). To reduce instrument noise effect on the spectrum measurement, canopy spectra were measured 10 times at each point, and the average values were used as the last results. To eliminate noise effects in the data, the reflectance data were smoothed using a weighted mean moving average over a 5 nm sample. This method provided sufficient smoothing to the reflectance data without loss of fine spectral detail information (Liao et al. 2013). Due to the strong absorption effect of vapor and carbon dioxide, 350-950 nm was selected as effective data for the subsequent analysis.

Measurement of Pigments and Leaf Area Index (LAI)

A portable SPAD-502 chlorophyll meter (Minolta, Spain) was used for the nondestructive measurements of leaf chlorophyll content. At each plot, the first and second leaves from the top of the wheat were measured 10 times each, and the average values were calculated as the final SPAD. However, to use the unit-less SPAD values for validating field-based leaf chlorophyll estimates, the SPAD value must be converted to leaf chlorophyll content. Previous research has shown that the determination of leaf chlorophyll content from the same SPAD-502 meter appears to be independent of species, which was theoretically justified by Markwell (Baret et al. 1991). Thus, we used the exponential equation developed by Markwell to convert SPAD-502 field measurements into leaf chlorophyll content ($\mu g/cm^2$):

$$C_{ab} = 6.34299 \cdot \exp\left(SPAD \cdot 0.04379\right) - 6.10629 \left(RMSD = 5.4\,\mu g / cm^2\right) \quad \ldots(1)$$

Here C_{ab} is the leaf chlorophyll content. *LAI*, which scales the leaf chlorophyll content from leaf to canopy levels, was measured using LAI-2000 Plant Canopy Analyzer (LI-COR, USA). The analyzer compares the light levels above and below the canopy, which were detected in five conical rings, to infer the LAI and characteristics of the canopy architecture (Jacquemoud et al. 2000). LAI-2000 was programmed to average four observations into a single value by using one measurement obtained above the canopy and four beneath the canopy: in the row, 1/4, 1/2, and 3/4 of the way across the row. This approach provided a good spatial average for row crops of partial cover. Then, the CCD was determined as

$$CCD = C_{ab} \cdot LAI \quad \ldots(2)$$

Here, the unit of CCD is g/m^2. We eventually acquired the CCD data of two complete growth stages for 77 samples in the jointing stage and 108 samples in the grain filling stage.

RESEARCH METHODOLOGY

Continuous Wavelet Transform (CWT)

Wavelet transform is a powerful signal processing tool that has been successfully used in remote sensing image processing to extract information from various scales (Simhadri et al. 1998); it includes two variations: discrete wavelet transform (DWT) and CWT (Dash et al. 2004). The CWT can decompose a signal at a continuum of positions, and CWT outputs can be easily interpreted. In this study, we used CWT to extract spectral information for CCD estimation.

The CWT is a linear operation that uses a mother wavelet function to convert a hyperspectral reflectance spectrum into sets of coefficients (Cheng et al.,2012). The main equation of wavelet transformation is as follows:

$$\psi_{a,b}(\lambda) = \frac{1}{\sqrt{a}}\psi\left(\frac{\lambda - b}{a}\right) \quad \ldots(3)$$

Here a and b are positive numbers. a represents the scaling factor defining the width of the wavelet and b is the shifting factor determining the position. The CWT output is given by (Cheng et al. 2014).

$$W_f(a,b) = \left\langle f, \psi_{a,b} \right\rangle = \int_{-\infty}^{+\infty} f(\lambda)\psi_{a,b}(\lambda)\, d_\lambda \quad \ldots(4)$$

Here $f(\lambda)(\lambda=1,2,\ldots, n, n$ is the number of spectral bands and herein $n = 601)$ is the reflectance spectrum. $W_f(a_i, b_j)$ $(i = 1,2,\cdots,m, j = 1,2,\cdots,n)$ represents the CWT coefficients. The CWT coefficients constitute a 2D scalogram, in which one dimension is scale and the other is wavelength. Previous research has reported that the shape of the absorption features of vegetation is similar to a Gaussian or quasi-Gaussian function (Combal et al. 2002). Therefore, the second derivative of Gaussian, also known as the Mexican hat, has been used as the mother wavelet basis (Broge et al. 2002, Combal et al. 2002). In the present study, the canopy spectra ranged from 350 nm to 950 nm, and 601 bands were available. Any scale greater than $2^9 = 512$ was discarded because decomposed components at high scales did not carry meaningful spectral information. All CWT operations were performed using Matlab 2010a (Natick, MA, USA).

Wavelet Feature Selection

A squared correlation coefficient (R^2) was calculated by the Pearson's linear correlations between elements of wavelet

Table 1: Spectral indices for predicting canopy chlorophyll density.

Spectral index	Acronym	Formula	Literature
Modified chlorophyll absorption reflectance index	*MCARI*	$\left[(R_{700} - R_{670}) - 0.2(R_{700} - R_{550})\right] / (R_{700}/R_{670})$	Daughtry et al.,2000
Simple ratio	*SR*	R_{NIR}/R_{Red}	Baret et al.,1991
Transformed chlorophyll absorption in reflectance index	*TCARI*	$3\left[(R_{700} - R_{670}) - 0.2(R_{700} - R_{550})\frac{R_{700}}{R_{670}}\right]$	Haboudane et al.,2002
Structure insensitive pigment index	*SIPI*	$(R_{800} - R_{445}) / (R_{800} - R_{680})$	Peñuelas et al.,1999
Chlorophyll index using green reflectance	CHL_{green}	$\frac{R_{760-800}}{R_{540-560}} - 1$	Gitelson et al.,2006
Chlorophyll index using red edge reflectance	$CHL_{red\ edge}$	$\frac{R_{760-800}}{R_{540-560}} - 1$	Gitelson et al.,2006
Modified normalized difference	*mND*705	$(R_{750} - R_{705}) / (R_{750} + R_{705} - 2R_{445})$	Sims et al.,2002
Normalized difference vegetation index	*NDVI*	$(R_{NIR} - R_{Red}) / (R_{NIR} + R_{Red})$	Rouse et al.,1973
Normalized pigment chlorophyll ratio index	*NPCI*	$(R_{680} - R_{430}) / (R_{680} + R_{430})$	Riedell et al.,1999
Photochemical reflectance index	*PRI*	$(R_{531} - R_{570}) / (R_{531} + R_{570})$	Gamon et al.,1997

Table 2: Descriptive statistics of CCD (g/m^2) at two growth stages of 2013.

Growth period	Number of plots	Mean ± s.d.	Min	Max	Coefficient of variation
Jointing stage	77	2.14±0.68	0.46	3.81	0.32
Grain filling stage	108	2.72±0.68	0.92	4.26	0.25
Two growth stages	185	2.48±0.74	0.46	4.26	0.30

power and CCD of all spectrum samples to identify features that are sensitive to variations in CCD. The most informative features for CCD were obtained by (1) retaining features where the correlations were statistically significant (P Value<0.0001) and (2) ranking these features in descending order on the basis of the R^2 values; a threshold was applied to delineate the top 1% features that mostly strongly correlated with CCD (Gitelson et al. 1996, Daughtry et al. 2000, Broge et al. 2002). These features formed several scattered feature regions. The feature with the maximum R^2 within each region was determined and expressed as (wavelength in nm, scale). Eventually, a small number of sparsely distributed features were selected as the optimal wavelet features related to changes in CCD.

Calculation of Spectral Indices

Several spectral indices specifically designed to quantify chlorophyll concentration were calculated (Table 1). These spectral indices were derived from previous studies that tested various species, leaf structures, developmental stages, and spectral indices (Gitelson et al. 2005, Blackburn et al. 2008, Ullah et al. 2012, Asner et al. 2008, Ollinger 2011). Broad-band spectral indices, such as *SR* and *NDVI*, were included because of their frequent use in monitoring vegetation status (Wu et al. 2014). The broad-band reflectance spectra of Landsat-5 TM were adopted as the standard for integrating original hyperspectral reflectance. In addition to the above-mentioned spectral indices, the other hyperspectral indices were calculated on the basis of the wavelengths given in the formulas.

Here, R_λ is the reflectance at wavelength λ.

RESULTS AND ANALYSIS

Growth stage variation in CCD and canopy reflectance properties

The CCD and canopy reflectance properties change as growth stages vary. Table 2 shows the descriptive statistics of CCD at two growth stages. The ranges of CCD are 0.46-3.81 g/m^2 and 0.92-4.26 g/m^2 for jointing and grain filling stages, respectively. The coefficient of variation of CCD in the jointing stage (32%) is higher than that in the grain filling stage (25%). At the two stages, the range of CCD is 0.46-4.26 g/m^2 and the coefficient of variation is 30%. This finding indicates that CCD varies widely along the two growth stages. Fig. 1 shows the average reflectance spectra from the jointing stage to the grain filling stage. Notably, the reflectance in the visible (350-713 nm) regions increases and decreases in the NIR (713-950 nm) regions.

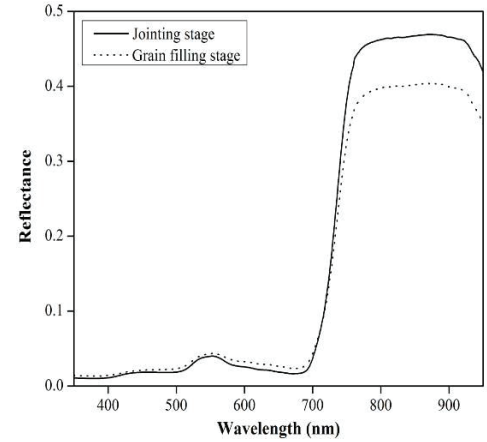

Fig. 1: Mean reflectance spectra at the jointing and grain filling stages.

Correlation of Spectral Indices with Canopy Chlorophyll Density

A correlation analysis was conducted between the 10 spectral indices from Table 1 and canopy chlorophyll density. Table

Table 3: Coefficient of determination between spectral indices and CCD (N=93).

Spectral indices	R	R^2	P Value	Spectral indices	R	R^2	P Value
SR	0.365	0.134	0.000	*mND705*	0.579	0.336	0.000
NDVI	0.533	0.284	0.000	*MCARI*	0.273	0.074	0.008
TCARI	0.053	0.003	0.612	CHL_{green}	0.059	0.003	0.574
NPCI	0.53	0.281	0.000	$CHL_{red\ edge}$	0.57	0.325	0.000
PRI	0.598	0.357	0.000	*SIPI*	0.503	0.253	0.000

Table 4: Correlations between CCD and most informative wavelet features derived from the calibration set (N=93)

Spectral metrics	Feature location		R	R^2	P Value
	Wavelength (nm)	Scale			
$WP_{513, 5}$	513	5	0.68	0.46	0.000
$WP_{730, 6}$	730	6	0.63	0.39	0.000
$WP_{800, 4}$	800	4	0.64	0.40	0.000
$WP_{835, 3}$	835	3	0.68	0.47	0.000
$WP_{897, 4}$	897	4	0.67	0.44	0.000

Table 5: Results of PLSR models based on wavelet features and spectral indices for the whole validation dataset and the dataset partitioned by growth stage.

Spectral metrics	Two stages			Jointing stage			Grain filling stage		
	R^2	RMSE	NRMSE	R^2	RMSE	NRMSE	R^2	RMSE	NRMSE
Wavelet features	0.64	0.43	23.6%	0.58	0.50	28.2%	0.61	0.39	24.6%
Spectral indices	0.57	0.48	25.8%	0.52	0.58	32.3%	0.59	0.40	25.2%

3 summarizes the results of the correlation analysis. Seven optimal spectral indices, namely, *SR*, *NDVI*, *NCPI*, *PRI*, *mND*705, $CHL_{red\ green}$ and *SIPI*, have a significant relationship with canopy chlorophyll density (P Value<0.0001). By contrast, *TCARI*, *MCARI* and CHL_{green} show low correlation with CCD.

Wavelet Features from CWA

Five most informative wavelet feature ranges, namely, 512-515 nm, 728-732 nm, 790-804 nm, 834-836 nm, and 892-902 nm, are determined in each scale after spectral data are processed by CWA. Features with the maximum R^2 within each region, namely, (513 nm, scale 5), (730 nm, scale 6), (800 nm, scale 4), (835 nm, scale 3), and (897 nm, scale 4), are determined in the visible and near infrared regions. They are highly sensitive to CCD (P Value<0.0001) with R^2 values for the linear regression ranging from 0.39 to 0.47 (Table 4). Low-scale features (835 nm, scale 3), (800 nm, scale 4), and (897 nm, scale 4) capture narrow absorption features in the near infrared region that are influenced by pigment concentration (Gitelson et al. 2005). Feature (513 nm, scale 5) occurs on the left shoulder of the green peak and captures spectral variation in the green range. High-scale feature (730 nm, scale 6) captures broad absorption features that occur in the range of red edge absorptions (Gitelson et al. 2005, Gitelson et al. 1996, Houborg et al. 2007). The R^2 and p values show that the five informative wavelet features perform better than the spectral indices in estimating CCD.

Regression model and validation of CCD using wavelet features and spectral indices

The PLSR model 1 was constructed with the five most informative wavelet features, while the PLSR model 2 was established with the seven optimal spectral indices of significant correlation with CCD. Table 5 summarizes the results of the two PLSR models for the whole validation dataset and the dataset partitioned by growth stage. In the two growth stages, the PLSR model 1 (R^2 = 0.64, RMSE=0.43 g/m^2, NRMSE=23.6%) is better than the PLSR model 2 (R^2= 0.57, RMSE=0.48 g/m^2, NRMSE=25.8%) in estimating CCD. After the validation data are partitioned by growth stage, the prediction accuracy of the two PLSR models exhibits low R^2 values and high NRMSE values. The PLSR model 1 has R^2 =0.58 and NRMSE=28.2% for the jointing stage and R^2 = 0.61 and NRMSE=24.6% for the grain filling stage. The PLSR model 2 has R^2 =0.52 and NRMSE=32.3% for the jointing stage and R^2 =0.59 and NRMSE=25.2% for the grain filling stage. The two PLSR models exhibit highly contrasting predictive capabilities in the growth stage and always have substantially better performance in the grain filling stage than in the jointing stage. This result is partly due to that winter wheat is in the rapid growth phase at the jointing stage. The signals are more easily contaminated by the background with the lower LAI in the jointing stage than in the grain filling stage, and the coefficient of variation of CCD in the jointing stage (32%) is also higher than that in the grain filling stage (25%). Therefore, the CWA method can remove the effects of background spectral variation when quantifying concentrations of components from mixtures (Mittermayr et al. 2001). This capability can be due to that the prediction accuracy of the PLSR model 1 is better than that of the PLSR model 2 in the jointing stage. Therefore, wavelet features are more robust than spectral indices. Fig. 2 plots the measured CCD against the estimated CCD for

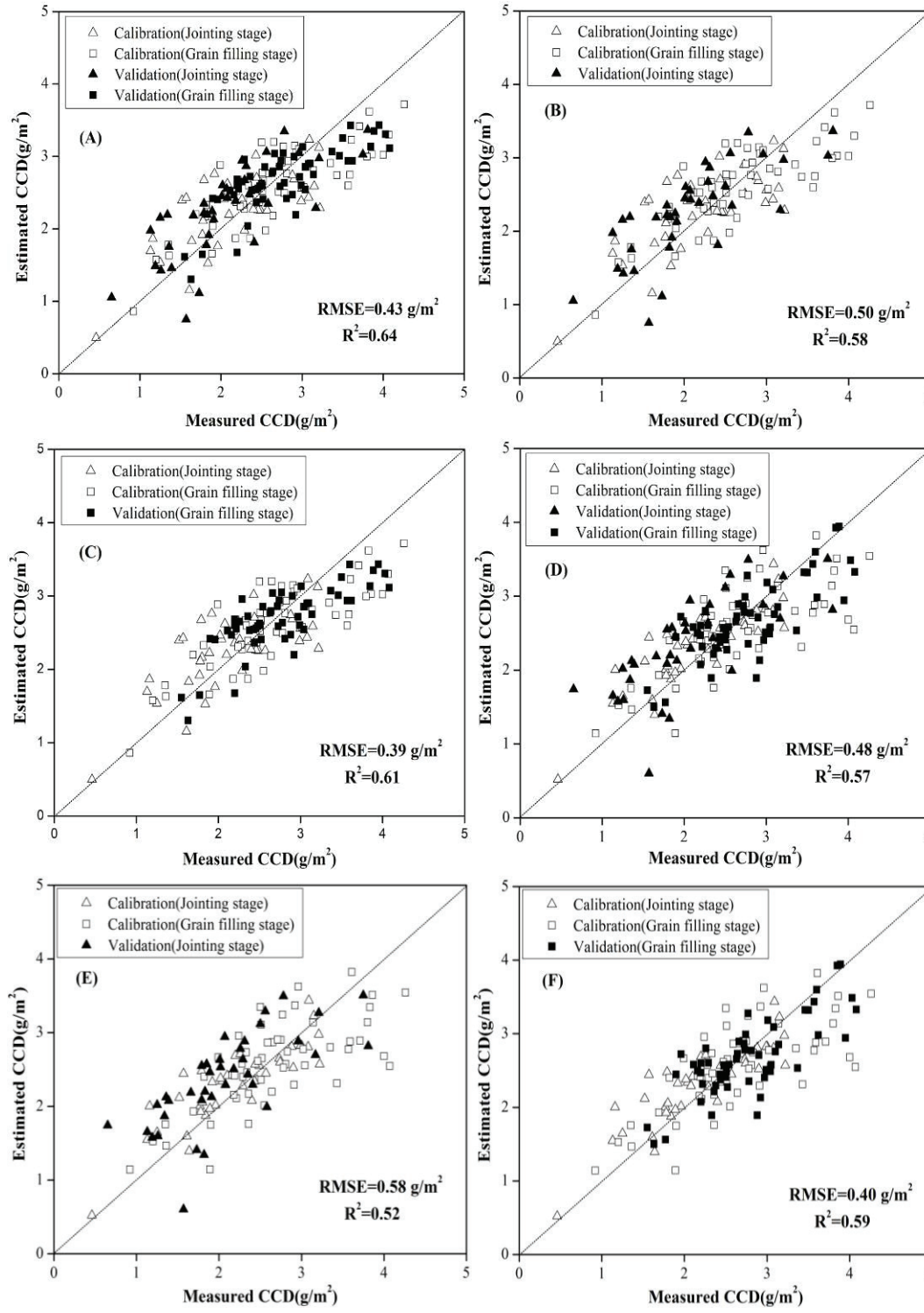

Fig.2: Plots of measured versus estimated CCD at the whole validation dataset (A and D), jointing stage (B and E), and grain filling stage (C and F) using PLSR model 1 (A, B, and C) and PLSR model 2 (D, E, and F). The predicted R^2, RMSE, and NRMSE values shown are obtained from the validation dataset.

illustrating the comparison of results and making them convincing. Ideally, the 1:1 line should be a perfect match. The figure indicates that the PLSR model 1 has points that are more convergent to the line 1:1 than the PLSR model 2 for the whole validation dataset and the dataset partitioned by growth stage. This condition indicates that the relationships between reflectance measures and CCD have been improved by the CWA method. Therefore, the CWA method can derive more robust wavelet features than the spectral indices for estimating CCD of winter wheat across different growth stages from the canopy spectra.

DISCUSSION AND CONCLUSION

This study presents the application of CWA method to canopy spectra for estimating CCD of winter wheat at two different growth stages. The CWA approach can effectively capture the meaningful spectral information that relates to CCD after the reflectance spectra are decomposed into various scales. Five most informative wavelet features, namely, (513 nm, scale 5), (730 nm, scale 6), (800 nm, scale 4), (835 nm, scale 3), and (897 nm, scale 4), are identified in the visible and near infrared regions. They are highly sensitive to CCD. Meanwhile, seven optimal spectral indices, namely, *SR*, *NDVI*, *NPCI*, *PRI*, *mND*705, $CHL_{red\ edge}$ and *SIPI* significantly correlate with CCD. They are used for further analysis. The PLSR model with the five wavelet features produces promising accuracy in estimating CCD. Specifically, the model has R^2 of 0.64, RMSE of 0.43 g / m^2, and NRMSE of 23.6%. Meanwhile, the PLSR model with seven optimal spectral indices produces less prediction accuracy of CCD. In particular, it has R^2 of 0.57, RMSE of 0.48 g / m^2, and NRMSE of 25.8%. After the validation dataset is partitioned into jointing and grain filling stages, the prediction accuracy of the two PLSR models exhibits low R^2 values and high NRMSE values. However, the PLSR model based on wavelet features still outperforms the model based on optimal spectral indices. Therefore, wavelet features are more effective than spectral indices in predicting CCD of winter wheat at different growth stages from canopy spectra for an agricultural ecosystem.

Our study extends the continuous wavelet analysis methodology to estimate chlorophyll content from leaf scale to canopy scale and exhibits promising results. However, winter wheat is the main crop in the study area. Thus, we only use winter wheat in this research. The capability of CWA in estimating CCD should be tested in the future using an extensive dataset with different crop species or at field scale with onboard hyperspectral images.

ACKNOWLEDGEMENTS

This research was supported by Doctoral Fund of Henan Institute of Engineering (D2016005). The authors are grateful to the staff of Beijing Normal University and Beijing Research Center for Information Technology in Agriculture for their support during field data collection.

REFERENCES

Asner, G.P. and Martin, R.E. 2008. Spectral and chemical analysis of tropical forests: Scaling from leaf to canopy levels. Remote Sensing of Environment, 112(10): 3958-3970.

Atzberger, C. 2004. Object-based retrieval of biophysical canopy variables using artificial neural nets and radiative transfer models. Remote Sensing of Environment, 93(1-2): 53-67.

Baret, F. and Guyot, G. 1991. Potentials and limits of vegetation indices for LAI and APAR assessment. Remote Sensing of Environment, 35(2-3): 161-173.

Blackburn, G.A. and Ferwerda, J.G. 2008. Retrieval of chlorophyll concentration from leaf reflectance spectra using wavelet analysis. Remote Sensing of Environment, 112(4): 1614-1632.

Boegh, E., Søgaard, H., Broge, N., Hasager, C.B., Jensen, N.O., Schelde, K. and Thomsen, A. 2002. Airborne multispectral data for quantifying leaf area index, nitrogen concentration, and photosynthetic efficiency in agriculture. Remote Sensing of Environment, 81(2-3): 179-193.

Broge, N.H. and Mortensen, J.V. 2002. Deriving green crop area index and canopy chlorophyll density of winter wheat from spectral reflectance data. Remote Sensing of Environment, 81(1): 45-57.

Buschmann, C. and Nagel, E. 1993. In vivo spectroscopy and internal optics of leaves as basis for remote sensing of vegetation. International Journal of Remote Sensing, 14(4): 711-722.

Cheng, T., Riaño, D. and Ustin, S.L. 2014. Detecting diurnal and seasonal variation in canopy water content of nut tree orchards from airborne imaging spectroscopy data using continuous wavelet analysis. Remote Sensing of Environment,143: 39-53.

Cheng, T., Rivard, B., Sánchez-Azofeifa, A.G., Féret, J.B., Jacquemoud, S. and Ustin, S.L. 2012. Predicting leaf gravimetric water content from foliar reflectance across a range of plant species using continuous wavelet analysis. Journal of Plant Physiology,169(12): 1134-1142.

Colombo, R., Bellingeri, D., Fasolini, D. and Marino, C.M. 2003. Retrieval of leaf area index in different vegetation types using high resolution satellite data. Remote Sensing of Environment, 86(1): 120-131.

Combal, B., Baret, F., Weiss, M., Trubuil, A., Mace, D., Pragnere, A., Myneni, R., Knyazikhin, Y. and Wang, L. 2002. Retrieval of canopy biophysical variables from bidirectional reflectance using prior information to solve the ill-posed inverse problem. Remote Sensing of Environment, 84(1): 1-15.

Dash, J. and Curran, P.J. 2004. The MERIS terrestrial chlorophyll index. International Journal of Remote Sensing, 25(23): 5403-5413.

Daughtry, C.S.T., Walthall, C.L., Kim, M.S., De Colstoun, E.B. and McMurtrey Iii, J.E. 2000. Estimating corn leaf chlorophyll concentration from leaf and canopy reflectance. Remote Sensing of Environment,74(2): 229-239.

Gamon, J.A., Serrano, L. and Surfus, J.S. 1997. The photochemical reflectance index: an optical indicator of photosynthetic radiation use efficiency across species, functional types and nutrient levels. Oecologia, 112(4): 492-501.

Gitelson, A.A., Vina, A., Ciganda, V., Rundquist, D.C. and Arkebauer, T.J. 2005. Remote estimation of canopy chlorophyll content in crops. Geophysical Research Letters, 32(8): L08403.

Gitelson, A.A., Kaufman, Y. and Merzlyak, M.N. 1996. Use of green channel in remote sensing of global vegetation from EOS-MODIS. Remote Sensing of Environment, 58(3): 289-298.

Gitelson, A.A., Keydan, G.P. and Merzlyak, M.M. 2006. Three-band model for noninvasive estimation of chlorophyll, carotenoids and anthocyanin

contents in higher plant leaves. Geophysical Research Letters, 33(11): L11402 .

Gitelson, A.A., Merzlyak, M. and Lichtenthaler, H. 1996. Detection of red edge position and chlorophyll content by reflectance measurements near 700 nm. Journal of Plant Physiology, 148(3-4): 501-508.

Haboudane, D., Miller, J.R., Tremblay, N., Zarco-Tejada, P.J. and Dextraze, L. 2002. Integrated narrow-band vegetation indices for prediction of crop chlorophyll content for application to precision agriculture. Remote Sensing of Environment, 81(2-3): 416-426.

Houborg, R. and Boegh, E. 2008. Mapping leaf chlorophyll and leaf area index using inverse and forward canopy reflectance modeling and SPOT reflectance data. *Remote Sensing of Environment*, 112(1): 186-202.

Houborg, R., Soegaard, H. and Boegh, E. 2007. Combining vegetation index and model inversion methods for the extraction of key vegetation biophysical parameters using Terra and Aqua MODIS reflectance data. Remote Sensing of Environment, 106(1): 39-58.

Jacquemoud, S., Bacour, C., Poilve, H. and Frangi, J.P. 2000. Comparison of four radiative transfer models to simulate plant canopies reflectance: Direct and inverse mode. Remote Sensing of Environment, 74(3): 471-481.

Liao, Q., Wang, J., Yang, G., Zhang, D., Lii, H., Fu, Y. and Li, Z. 2013. Comparison of spectral indices and wavelet transform for estimating chlorophyll content of maize from hyperspectral reflectance. Journal of Applied Remote Sensing, 7(1): p. 073575.

Mittermayr, C.R., Tan, H.W. and Brown, S.D. 2001. Robust calibration with respect to background variation. Applied Spectroscopy, 55(7): 827-833.

Nijs, I., Behaeghe, T. and Impens, I. 1995. Leaf nitrogen content as a predictor of photosynthetic capacity in ambient and global change conditions. Journal of Biogeography, 22(2): 177-183.

Ollinger, S.V. 2011. Sources of variability in canopy reflectance and the convergent properties of plants. New Phytologist, 189(2): 375-394.

Peñuelas, J. and Inoue, Y. 1999. Reflectance indices indicative of changes in water and pigment contents of peanut and wheat leaves. Photosynthetica, 36(3): 355-360.

Riedell, W.E. and Blackmer, T.M. 1999. Leaf reflectance spectra of cereal aphid-damaged wheat. Crop Science, 39(6): 1835-1840.

Rouse Jr, J., Haas, R.H., Schell, J.A. and Deering, D.W. 1973. Monitoring vegetation systems in the great plains with ERTS. Proceedings of the Third ERTS Symposium, Washington DC, 10-14 December, 309-317.

Simhadri, K.K., Iyengar, S.S., Holyer, R.J., Lybanon, M. and Zachary, J.M. 1998. Wavelet-based feature extraction from oceanographic images. IEEE Transactions on Geoscience and Remote Sensing, 36(3): 767-778.

Sims, D.A. and Gamon, J.A. 2002. Relationships between leaf pigment content and spectral reflectance across a wide range of species, leaf structures and developmental stages. Remote Sensing of Environment, 81(2-3): 337-354.

Ullah, S., Skidmore, A.K., Naeem, M. and Schlerf, M. 2012. An accurate retrieval of leaf water content from mid to thermal infrared spectra using continuous wavelet analysis. Science of the Total Environment, 437: 145-152.

Wu, J., Hou, L.G. and Wang, D. 2014. Estimation of chlorophyll content of corn canopy based on hyperion image. Transactions of the Chinese Society of Agricultural Engineering, 30(6): 116-123.